Research paper

The risk matrix of vector-borne diseases in metapopulation networks and its relation with local and global R_0

A. Anzo-Hernández [b,*], B. Bonilla-Capilla [b], J. Velázquez-Castro [a], M. Soto-Bajo [b], A. Fraguela-Collar [a]

[a] *Facultad de Ciencias Físico-Matemáticas, Benemérita Universidad Autónoma de Puebla, Avenida San Claudio y 18 Sur, Colonia San Manuel, 72570, Puebla, México*
[b] *Cátedras CONACYT - Benemérita Universidad Autónoma de Puebla Facultad de Ciencias Físico-Matemáticas, Benemérita Universidad Autónoma de Puebla, Avenida San Claudio y 18 Sur, Colonia San Manuel, 72570, Puebla, México*

ABSTRACT

The basic reproduction number R_0 is an index worldwide commonly used by public health organizations as a key estimator of the severity of a given epidemic. In this work we use a Lagrangian approach to model vector-borne diseases (SIR-SI) into a metapopulation network in order to derive an expression of the basic reproduction number and we analyze its dependency on human mobility. We prove that this index can be computed by evaluating the spectral radius of the risk matrix W, whose entries W_{ij} are the number of secondary cases in patch j produced by the inclusion of a single infected human in patch i. Based on the risk matrix, we propose a risk index which locally describes the epidemic vulnerability, while R_0 give us an estimation of the global vulnerability. Further, we numerically analyze the effect of human mobility over the values of R_0 in a system composed of two and three patches, and for a network connected in a star topology configuration.

© 2018 Elsevier B.V. All rights reserved.

1. Introduction

Vector-borne diseases, particulary those transmitted by mosquitoes, are one of the most important concerns in public health, mainly due to its growing impact and fast spreading in endemic areas. In particular, Dengue (DEN), Zika (ZIKV) and Chikungunya (CHIKV) are the main three arboviruses that are transmitted to humans via the bite of two mosquito species (among the 3500 mosquito species in the world) named *Aedes aegypti* (*Stegomyia aegypti*), which is adapted to a peri-domestic environment and urban areas [1]), and *Aedes albopictus* (*Stegomyia albopicta*). For instance, Dengue arbovirus causes approximately 100 million annually at worldwide level, mostly in tropical and sub tropical countries [2]. In addition, according to the World Health Organization [3], in June 2016, 61 countries reported cases of ZIKV disease, and in May 2017 such a number grew up to 84. Currently, CHIKV have received considerable public health attention due to its recently incursion in the Americas, with 146,914 confirmed cases in 2016 [4].

How and where a vector-borne disease will occur is one of the main research problems in epidemiology. Since these mosquitoes rarely travel long distances (the maximum dispersa of *Aedes aegypti* is ten meters and, *Aedes albopictus* one is

---

* Corresponding author.
E-mail addresses: andres.anzo@fcfm.buap.mx (A. Anzo-Hernández), beatriz.bonillac@correo.buap.mx (B. Bonilla-Capilla), jorge.velazquezcastro@correo.buap.mx (J. Velázquez-Castro), moises.soto@fcfm.buap.mx (M. Soto-Bajo), fraguela@fcfm.buap.mx (A. Fraguela-Collar).

400–600 m [5]), one of the key factors to amplify or dampen a disease outbreak is the mobility of people among different spatial regions [6–8,11,12]. Take as an example the recent spread of ZIKV in Americas, which according to the analysis presented in [13], it is estimated that the first introduction of ZIKV occured in Brazil between the Soccer Confederation Cup in 2013 and the Soccer World Cup in 2014, and the subsequent spread over 47 countries was caused by the daily human flow [13]. This reflects the importance of incorporate, in the classical SIR epidemiological models, the human mobility among different geographical zones, ranging from urban areas inside a city to global tracks between countries.

In this context, the metapopulation models, widely used in Ecology [14], have been considered in the study of disease outbreaks. An early work in this direction can be traced back to the model of sexually transmitted diseases presented by Arino and van den Driessche [15], which were extended later to other types of diseases as those transmitted by mosquitoes [16].

In order to formulate a metapopulation network model, firstly the geographic territory is partitioned into patches, each one occupied by individuals; next one consider a network of patches by adding links among them if humans of a given patch moves towards another patch. Currently, there are two perspectives about how to model mobility of humans in a network of patches [8]: in the first one, named the Eulerian approach, people emigrate into a neighboring patch in which they settle as new residents. In the second one, named the Lagrangian approach, people spend a fraction of their day at some patch (by work or personal reasons) and then return to its own patch after that. Because of the features of a vector-borne disease, in this work we make use of the Lagrangian approach, from which human mobility is described by the dwell-time parameters p_{ij}, that stand for the fraction of the day that residents from patch i spend in patch j [5,17]. It is worth mentioning that agent-based models (ABM) are another methodology currently used to analyze vector borne diseases in metapopulations models [9]. Such models let us track spatial and temporal factors like population density and dynamics in heterogeneous populations. However, ABM requires significant computing resources.

An important quantity in Epidemiology is the basic reproduction number R_0. This quantity represents the secondary cases generated by an individual inside a totally susceptible population [20]. In simple single patch epidemic models this quantity can be derived from the stability analysis of the system, but it can also be calculated directly from the model and its meaning [10]. With the stability analysis it is also proved that if $R_0 < 1$, then the disease-free equilibrium (DFE) state is asymptotically stable, and unstable if $R_0 > 1$ [19]. In multi-patch models the traditional interpretation of R_0 is not valid anymore because the secondary cases generated by the insertion of an infected individual depend on the patch of insertion. For this reason, in multi-patch models it becomes necessary to employ the NGM methodology. This method consists in decomposing the Jacobian matrix into two matrices called the transmission and transition parts; from which the NGM is determined [20]. R_0 is then the spectral radius of the NGM. In this models R_0 is used to indicate when the disease free equilibrium is stable or unstable [18]. On the other hand, Keeling and Rohani [10] gave a biological interpretation of this value as "the average number of secondary cases arising from an average infected individual in an entirely susceptible population, once initial transients have decayed". Even with this interpretation, it is difficult to calculate R_0 directly from the model and even more from a vector borne disease.

An analysis and an inspiring work for our research is the result presented by Bichara and Castillo-Chavez in [5]. There, a metapopulation network model for vector-borne diseases is proposed assuming a SIS epidemic model for humans and a SI framework for mosquitoes, and considering that the network is composed by N human groups and M patches occupied just by mosquitoes. That is, the system is a bipartite network from which an expression of R_0 is obtained in terms of the spectral radius of products of matrices. Further, it is also shown in [5] that the DFE state is globally asymptotically stable (GAS) if $R_0 < 1$, and the endemic equilibrium state is GAS if $R_0 > 1$, under the assumption that the dwell-time matrix $\mathbf{P} = [p_{ij}]_{N \times N}$ is irreducible.

On the other hand, based on the Bailey - Dietz model, which considers a metapopulation system with human migration, Iggidr et al. [21] distinguish three different R_0 involved in this type of systems: (a) the global one derived from the NGM methodology, (b) the uniform one, obtained by assuming that the patches are homogenous, and (c) the local one (which we denote as R_{0i}, with i the label of the patch), obtained when the patches were disconnected. Furthermore, the authors in [21] derive an expression for R_0 assuming that the mobility time-scale within the patch is larger than when it is compared to either the demographic or epidemiological time scales, where some additional parameters are included such as the vector alternative blood sources.

In this same direction but assuming a reduced system of two connected patches, Lee and Sunmi [22] consider a SEIR (Susceptible - Exposed - Infected - Recovered) framework for humans and a SEI for mosquitoes, and analyze three human mobility scenarios: (i) unidirectional motion, (ii) symmetric bidirectional, and (iii) asymmetric bidirectional motion. In other words, they fix the values of the dwell-time parameters p_{ij} while varying the local reproduction numbers R_{0i} and R_{0j} in order to show that larger asymmetry in the mobility patterns lead to larger final epidemic sizes.

In this paper we show that for vector-borne diseases R_0 can be found as the spectral radius of a risk matrix W of dimension $N \times N$. This allows to greatly reduce the computational difficulty of finding R_0. In addition to this, we give an interpretation for the elements of W making it possible to calculate them directly from the model. Specifically, the entries W_{ij} are the secondary infection cases that are generated in patch j due to the inclusion of a single infected human in patch i and because of the human mobility among patches. In this sense, the risk matrix describes the mobility influence of a given patch over the propagation of a vector-borne disease in the entire metapopulation network.

In order to show these results, we used a specific model where the dynamics of each patch is described by a compartment SIR model for humans and SI for vectors. Two patches are connected if humans travel between them; that is, from the

Lagrangian approach, we assume that the dynamical network is connected with weighted and directional links described by the dwell-time parameters p_{ij}.

Once having the expression for R_0, we numerically analyze the case of two patches, where we explore three possible scenarios: (a) the local basic reproduction number of patch i is $R_{0i} > 1$ and $R_{0j} < 1$; (b) both indices are smaller than one; and (c) both are bigger than one. We find the values of p_{ij} for which the disease outbreak is triggered or not in each patch. Next we extend this study to the case in which a third patch, with label k and local basic reproduction number $R_{0k} > 1$, is connected to the above system of two patches. Here we analyze the effect of the out-flow and in-flow of humans in the new patch k and we observe that the in-flow can produce a major number of secondary infection cases in the entire metapopulation network. We found two potential effects of human mobility in a system. The first one is that it can trigger a disease outbreak in a metapopulation ($R_0 > 1$) even if for the same patches but without human mobility there isn't an outbreak, i.e. $R_{0i} < 1$, $\forall i$. The second one is that in certain cases, human mobility can dampen a disease outbreak ($R_0 < 1$) compared to the same isolated patches, *i.e.* $\exists\ i$ such that $R_{0i} > 1$. Finally, we study the case of N patches connected in a star topology configuration and we find the values for the dwell-time parameters that can reduce the number of infected humans in the central patch.

This paper is organized as follows: in Section 2 we present some preliminaries. Specifically, we describe a single population model with the SIR-SI epidemic model for vector-borne diseases. Next, we use this model to describe the NGM methodology. In Section 3 we find the basic reproduction number for a metapopulation network connected in an arbitrary topology configuration. In Section 4 we analyze numerically the effect of the mobility for a system of two and three patches, and for a metapopulation network with a star topology configuration. Further, we assess the basic reproduction number for each one of the above examples by varying the dwell-time parameters. In Section 5 we present some concluding remarks.

2. R_0 for a single and isolated patch

With the aim of deriving a mathematical model for a metapopulation network with human mobility, first we describe the compartmental local model SIR-SI which describes the vector-borne disease dynamics of an isolated patch; i.e., when it is not connected to the network. Taking this model into account, we obtain the expression of the local basic reproduction number following the NGM methodology.

2.1. Single population model

Consider an isolated patch i occupied by a homogeneously mixing population of N_{hi} humans and N_{vi} vectors. Furthermore, assume that human population is classified at every time instant t as susceptible $S_i(t)$, infected $I_i(t)$, and recovered $R_i(t)$ (with $N_{hi} = S_i(t) + I_i(t) + R_i(t)$ $\forall t$), while vector population can be classified into susceptible $M_i(t)$ and infected $V_i(t)$ (with $N_{vi}(t) = M_i(t) + V_i(t)$). Other compartments can be incorporated to the model, as for example the exposed hosts or vectors in aquatic phase, which includes egg, larva and pupa states [23]. In this paper we do not incorporate other compartments because we are more interested in the general properties of vector-borne diseases. Hence we use a SIR (Susceptible-Infected-Recovered) model for humans and a SI model for vectors, given by the following set of nonlinear differential equations:

$$
\text{humans}
\begin{cases}
\dot{S}_i = \mu_{hi}(N_{hi} - S_i) - \beta_i V_i \dfrac{S_i}{N_{hi}}\,, \\[2mm]
\dot{I}_i = -(\gamma_i + \mu_{hi})I_i + \beta_i V_i \dfrac{S_i}{N_{hi}}\,, \\[2mm]
\dot{R}_i = \gamma_i I_i - \mu_{hi} R_i\,,
\end{cases}
\tag{1}
$$

$$
\text{vectors}
\begin{cases}
\dot{M}_i = \Lambda_i - \mu_{vi} M_i - \beta_i M_i \dfrac{I_i}{N_{hi}}\,, \\[2mm]
\dot{V}_i = -\mu_{vi} V_i + \beta_i M_i \dfrac{I_i}{N_{hi}}\,.
\end{cases}
\tag{2}
$$

Here, β_i is the number of vector bites per human per time unit. Then, $\beta_i V_i S_i / N_{hi}$ is the total number of susceptible hosts that become ill by the bite of the infected vectors, and $\beta_i M_i I_i / N_{hi}$ is the total number of susceptible vectors that contract the arbovirus due to their interaction with the fraction I_i / N_{hi} of infected hosts. On the other hand, μ_{hi} and μ_{vi} are the per-capita birth and natural mortality rates in humans and vectors respectively, and γ_i is the per-capita human recovery rate. In this model we assume that the natural growth of susceptible vectors is described by the constant recruitment rate Λ_i. In Table 1 we present some numerical values from the above described parameters reported in the literature for the Dengue case [24,25].

In order to illustrate the dynamics of the vector-borne disease for a single and isolated patch, we show in Fig. 1 the numerical solution of the SIR-SI model (1) and (2), by using the fourth order Runge – Kutta method (RK4) and the parameters values given in Table 1, with $\beta = 0.67$, and initial condition $S_i(t = 0) = 10,000$, $I_i(t = 0) = 1$, $R_i(t = 0) = 0$, $M_i(t = 0) = 8,000$, $V_i(t = 0) = 0$.
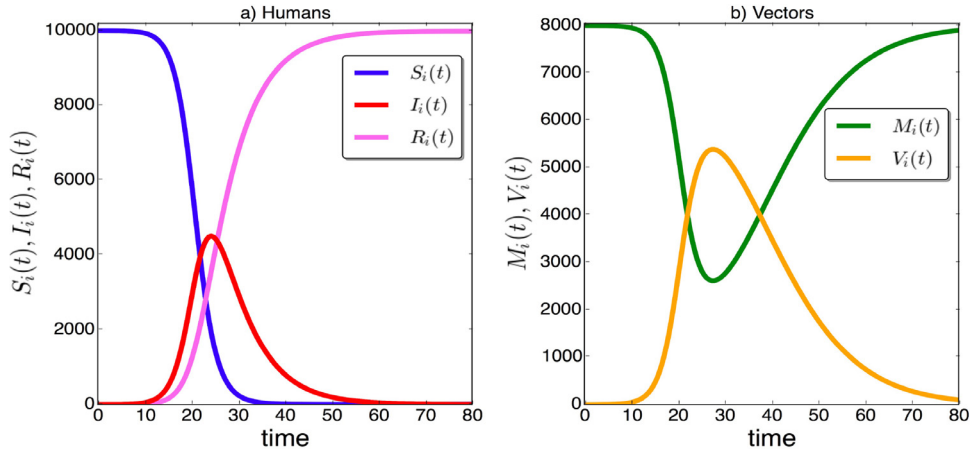
Fig. 1. Numerical solution of the SIR-SI model (1) and (2) with the fourth order Runge–Kutta method (RK4) and with the parameters values given in Table 1; with $\beta_i = 0.67$, and initial condition $S_i(t = 0) = 10,000$, $I_i(t = 0) = 1$, $R_i(t = 0) = 0$, $M_i(t = 0) = 8000$, $V_i(t = 0) = 0$.

Table 1
Description and parameters values of the SIR-SI model (Eqs. (1) and (2)) for the Dengue case [24,25].

Parameter	Description	Numerical value
μ_{hi}	Per-capita birth/mortality rate of humans (per day, per capita)	4.57×10^{-5} humans/days
μ_{vi}	Per-capita mortality rate of adult female mosquitoes (per day, per capita)	1/8 mosquitos/days
γ_i	Humans recovery rate (per day, per capita)	1/7 humans/days
Λ_i	The constant recruitment rate of vectors	1000 mosquitoes/days
β_i	Effective vector biting rate (global number of bites, per day, per mosquito)	[0.2,0.67] bites/mosquitoes × days

2.2. Computing the local R_{0i} with the NGM methodology

The key idea in the Next Generation Matrix (NGM) methodology is interpreting the infection process as a demographic one with consecutive generations of infected individuals. Such a process can be characterized by the NGM, since the basic reproduction number is defined as the spectral radius of the NGM [20]. In what follows we briefly explain this methodology using the SIR-SI model (1) and (2) as an example. In order to distinguish between the basic reproduction number for a metapopulation network and the basic reproduction number of a single patch (when it is isolated from the network), we denote with R_{0i} the local basic reproduction number of the ith patch.

The first step consists in separating the compartmental model into two subsystems: infected compartments, also named the infected subsystem, and the disease-free subsystem. For the SIR-SI model (1) and (2), the infected subsystem is composed by the state variables $x = (x_1, x_2) = (I_i, V_i) \in \mathbf{R}^2$, while the state variables $y = (S_i, R_i, M_i) \in \mathbf{R}^3$ correspond to the disease-free subsystem. Then the right-hand side of the infected subsystem is split as follows:

$$\dot{I}_i = -\underbrace{\sigma_{hi}I_i}_{\mathcal{H}_1(x,y)} + \underbrace{\beta_i V_i S_i^*}_{\mathcal{T}_1(x,y)}, \quad \text{and} \quad \dot{V}_i = -\underbrace{\mu_{vi}V_i}_{\mathcal{H}_2(x,y)} + \underbrace{\beta_i M_i I_i^*}_{\mathcal{T}_2(x,y)}, \tag{3}$$

where we have defined $\sigma_{hi} = \gamma_i + \mu_{hi}$, $S_i^* = S_i/N_{hi}$, and $I_i^* = I_i/N_{hi}$ in order to reduce the notation. Here, $\mathcal{H}_k$ (for $k = 1, 2$) incorporates the transition terms (births, deaths, disease progression, and recovery), while $\mathcal{T}_k$ is the rate of appearance of new infections (*i.e* the transmission term) [26]. The selection of the transition and transmission terms of Eq. (3) should be performed by considering the following assumptions [19,26]:

- $\mathcal{H}_k(0, y) = 0$ and $\mathcal{T}_k(0, y) = 0$, for all $y > 0$ and $k = 1, 2$. That is, the first condition says that there is no immigration from disease-free subsystem to the infected one; and the second condition states that all new infections arise from the infected compartment only.
- $\mathcal{H}_k(x, y) \leq 0$ whenever $x_k = 0$ for $k = 1, 2$. The above says that each element of the transitional term represents the net outflow and must be negative (inflow only).
- $\mathcal{T}_k(x, y) \geq 0$ for all nonnegative x and y, and $k = 1, 2$. This means that new infections can only be produced.
- $\sum_{k=1}^{2} \mathcal{H}_k(x, y) \geq 0$ for all nonnegative x and y, *i.e.* the total outflow of all infected compartments is nonnegative.
- The disease-free subsystem (corresponding to $I_i = V_i = 0$) has an unique equilibrium point $(S_i, R_i, M_i) = (N_{hi}, 0, \Lambda_i/\mu_{vi})$ which is globally asymptotically stable.
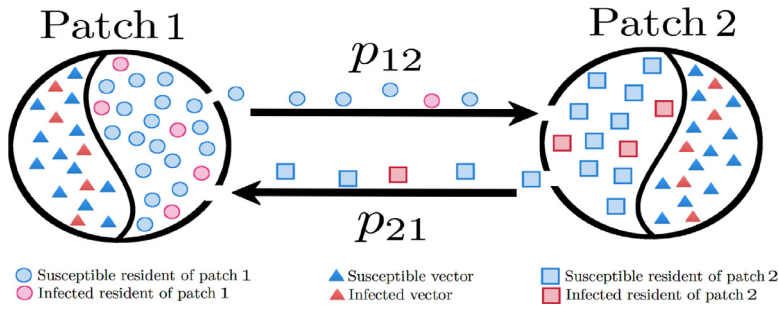
Fig. 2. Schematic representation of the interaction between two patches.

It is straightforward to show that the selection of the transition and transmission terms defined in (3) satisfy the above assumptions. Next, we compute the following matrices:

$$\mathcal{H} = \left[\frac{\partial \mathcal{H}_j}{\partial x_k}\bigg|_D\right]_{2\times 2} = \begin{pmatrix} \sigma_{hi} & 0 \\ 0 & \mu_{vi} \end{pmatrix}; \mathcal{T} = \left[\frac{\partial \mathcal{T}_j}{\partial x_k}\bigg|_D\right]_{2\times 2} = \beta_i \begin{pmatrix} 0 & 1 \\ \dfrac{\Lambda_i}{\mu_{vi} N_{hi}} & 0 \end{pmatrix}; \tag{4}$$

for $j, k = 1, 2,$ and where $D = (N_{hi}, 0, 0, \Lambda_i/\mu_{vi}, 0)$ is the disease-free equilibrium (DFE) state. The matrices $\mathcal{H}$ and $\mathcal{T}$ are called the transition and transmission matrices respectively. It is straightforward to note that the above process is equivalent to linearize the infected subsystem around the *DFE* state and rewrite the resulting Jacobian matrix as $J = \mathcal{T} - \mathcal{H}$.

The matrix $K = \mathcal{T}\mathcal{H}^{-1}$ is called the NGM [20] which, for the SIR-SI model (1) and (2) becomes:

$$K = \begin{pmatrix} 0 & \dfrac{\beta_i}{\mu_{vi}} \\ \beta_i \dfrac{\Lambda_i}{N_{hi}\sigma_{hi}\mu_{vi}} & 0 \end{pmatrix}.$$

Hence the local basic reproduction number is given by the spectral radius $\rho(K)$ of the NGM. Then, by using the characteristic polynomial $p(\lambda) = det(K - \lambda \mathbb{I}_2)$ (with $\mathbb{I}_2$ the 2×2 identity matrix) we get the following mathematical expression of R_{0i} (for the SIR-SI model (1) and (2)):

$$R_{0i} = \rho(K) = \beta_i \sqrt{\frac{\Lambda_i}{N_{hi}\sigma_{hi}\mu_{vi}^2}} \,. \tag{5}$$

For the parameters values given in Table 1, the local basic reproduction number for a single and isolated population is $R_{0i} = 4.48$. According to the results of Diekmann et al. [20], the DFE state is asymptotically stable if $R_{0i} < 1$ and, it is unstable otherwise.

In the next section we use this NGM methodology in order to get an expression of the basic reproduction number for a system of N connected patches.

3. R_0 for a metapopulation network and the risk matrix W

In order to get a mathematical expression for the basic reproduction number R_0 in a system of N connected patches, we first derive the model from the Lagrangian approach by assuming that the dynamics of each patch is given by the SIR-SI model (1) and (2) and the connection among patches is described by human mobility patterns. After that, we use the NGM methodology in order to derive an expression for the basic reproduction number R_0 of the metapopulation network.

3.1. Metapopulation network model

We consider a network composed of N patches, each one inhabited by an homogeneously mixing population of N_{hk} humans and N_{vk} vectors, where $k \in \{1, 2, \ldots, N\}$ is the patch label. Let $S_k(t), I_k(t), R_k(t)$ be the number of residents that are susceptible, infected and recovered; let $M_k(t)$ and $V_k(t)$ be the number of susceptible and infected vectors in the kth patch, respectively.

We assume that there exists a flux of human mobility among patches, while vectors remain in the same patch all the time (in Fig. 2 we draw an schematic representation of the human mobility between two patches). In order to incorporate human mobility in the SIR-SI model (1) and (2), we consider the dwell-time matrix $\mathbf{P} = [p_{ij}]_{N\times N}$, whose entries $p_{ij} \geq 0$, for $i, j = 1, \ldots, N$, describe the fraction of time during a day hosts in patch i spend in patch j [5,17]. The dwell-time matrix should satisfy $\sum_{j=1}^{N} p_{ij} = 1$ for all i.

The effect of human mobility in the spread of a vector-borne disease is introduced by substituting the last term at right hand of the Eq. (1) by the function f_k, which describes the human mobility over the metapopulation network of

susceptible residents from kth patch, and how they contract the arbovirus due to the bite of infected vectors that live in patches that they visit. Additionally, the last term at right hand of the Eq. (2) is replaced by the function g_k, which describes the human mobility over the metapopulation network of the infected residents from any patch, and how they interact with susceptible vectors in patch k. In this context, the SIR-SI model with human mobility between the N patches is expressed as the following system of $5N$ non-linear ordinary differential equations:

$$\text{Patch } k \begin{cases} \dot{S}_k = \mu_{hk}(N_{hk} - S_k) - f_k(S_k, \mathbf{I_v}), \\ \dot{I}_k = -(\gamma_k + \mu_{hk})I_k + f_k(S_k, \mathbf{I_v}), \\ \dot{R}_k = \gamma_k I_k - \mu_{hk}R_k, \\ \dot{M}_k = \Lambda_k - \mu_{vk}M_k - g_k(M_k, \mathbf{I_h}), \\ \dot{V}_k = -\mu_{vk}V_k + g_k(M_k, \mathbf{I_h}); \end{cases} \tag{6}$$

where $k = 1, 2, \ldots, N$ is the index that label each patch; μ_{hk}, μ_{vk}, γ_k and Λ_k are the parameters described in Table 1 for the kth patch; $\mathbf{I_v} = (V_1, V_2, \ldots, V_N)$ and $\mathbf{I_h} = (I_1, I_2, \ldots, I_N)$.

Let $w_{hi} = \sum_{\tau=1}^{N} p_{\tau i} N_{h\tau}$ be the effective number of humans that spend their time in patch i, including both own residents and visitors of the neighboring patches. We interpret w_{hi} as the tourist attraction of the patch i since it indicates the amount of humans that daily visit it. Then, the term $S_k p_{kj}/w_{hj}$ is the proportion of susceptible humans that travel from patch k to patch j and, $I_j p_{jk}/w_{hk}$ is the proportion of infected hosts of patch j that travel to patch k. With these terms we can define the functions f_k and g_k for patch k as:

$$f_k(S_k, \mathbf{I_v}) = \sum_{j=1}^{N} \beta_j V_j \frac{S_k p_{kj}}{w_{hj}}, \tag{7}$$

and

$$g_k(M_k, \mathbf{I_h}) = \sum_{j=1}^{N} \beta_k M_k \frac{I_j p_{jk}}{w_{hk}}. \tag{8}$$

The dynamical behavior of the metapopulation network (6) for $N = 2$, $N = 3$, and for $N = 6$ patches connected in a star topology configuration, and for different values of the dwell-time p_{ij}, it will be illustrated in the section Numerical examples. But before that, in the next section we compute the basic reproduction number R_0 using the NGM methodology described previously.

3.2. Computing R_0 with the NGM methodology

As we described in the previous section, in order to get the NGM we separate from the Eq. (6) the infected subsystem as follows:

$$\dot{I}_k = \underbrace{-\sigma_{hk}I_k}_{\mathcal{H}_{1k}} + \underbrace{f_k(S_k, \mathbf{I_v})}_{\mathcal{T}_{1k}},$$

$$\dot{V}_k = \underbrace{-\mu_{vk}V_k}_{\mathcal{H}_{2k}} + \underbrace{g_k(M_k, \mathbf{I_h})}_{\mathcal{T}_{2k}};$$

for $k = 1, \ldots, N$. Here, $\sigma_{hk} = \gamma_k + \mu_{hk}$. It is straightforward to show that the collection of transition functions $\mathcal{H}_{1k}$, $\mathcal{H}_{2k}$; and transmission functions $\mathcal{T}_{1k}$, $\mathcal{T}_{2k}$ satisfy the assumptions proposed in [19,26] and also described in the Section 2.2 of this paper. Then, the transition and transmission matrices are given by:

$$\mathcal{H} = \begin{bmatrix} \left[\frac{\partial \mathcal{H}_{1i}}{\partial I_j}\Big|_D\right]_{N \times N} & \left[\frac{\partial \mathcal{H}_{1i}}{\partial V_j}\Big|_D\right]_{N \times N} \\ \left[\frac{\partial \mathcal{H}_{2i}}{\partial I_j}\Big|_D\right]_{N \times N} & \left[\frac{\partial \mathcal{H}_{2i}}{\partial V_j}\Big|_D\right]_{N \times N} \end{bmatrix} = \begin{bmatrix} \text{diag}\{\sigma_{hi}\} & \mathcal{O}_N \\ \mathcal{O}_N & \text{diag}\{\mu_{vi}\} \end{bmatrix}_{2N \times 2N}$$

and

$$\mathcal{T} = \begin{bmatrix} \left[\frac{\partial \mathcal{T}_{1i}}{\partial I_j}\Big|_D\right]_{N \times N} & \left[\frac{\partial \mathcal{T}_{1i}}{\partial V_j}\Big|_D\right]_{N \times N} \\ \left[\frac{\partial \mathcal{T}_{2i}}{\partial I_j}\Big|_D\right]_{N \times N} & \left[\frac{\partial \mathcal{T}_{2i}}{\partial V_j}\Big|_D\right]_{N \times N} \end{bmatrix} = \begin{bmatrix} \mathcal{O}_N & [\eta_{ij}p_{ij}]_{N \times N} \\ [\kappa_i p_{ji}]_{N \times N} & \mathcal{O}_N \end{bmatrix}_{2N \times 2N}$$

for $i, j = 1, \ldots, N$. Here, $diag\{\sigma_{hi}\}$ is a $N \times N$ diagonal matrix, $\mathcal{O}_N$ is the null matrix of dimension N, $\eta_{ij} = \beta_j N_{hi}/w_{hj}$, and $\kappa_i = \beta_i \Lambda_i/\mu_{vi}w_{hi}$. Note that the DFE state is $D = (N_{h1}, 0, 0, \Lambda_1/\mu_{v1}, 0, \ldots, N_{hN}, 0, 0, \Lambda_N/\mu_{vN}, 0) \in \mathbf{R}^{5N}$.

Then, according to Diekmann et al. [20], the NGM is given by the following $2N \times 2N$ block matrix:

$$K = \mathcal{T}\mathcal{H}^{-1} = \begin{pmatrix} \mathcal{O}_N & B^h \\ B^v & \mathcal{O}_N \end{pmatrix}, \tag{9}$$

where $B^h = [\eta_{ij} p_{ij}/\mu_{vj}]_{N \times N}$ and $B^v = [\kappa_i p_{ji}/\sigma_{hj}]_{N \times N}$ for $i, j = 1, \ldots, N$.

Using the result given in [27,28] for the determinant of a block matrix, and the property $det(\alpha A) = \alpha^n det(A)$ with A a square $n \times n$ matrix and $\alpha \in \mathbf{R}$, we get the following characteristic polynomial of the NGM (9):

$$-p(\lambda) = \begin{vmatrix} \lambda \mathbb{I}_N & -B^h \\ -B^v & \lambda \mathbb{I}_N \end{vmatrix} = det \left| \lambda \mathbb{I}_N - B^h (\lambda \mathbb{I}_N)^{-1} B^v \right| det \left| \lambda \mathbb{I}_N \right| = det \left| \lambda^2 \mathbb{I}_N - W \right|.$$

Here, $\mathbb{I}_N$ is the $N \times N$ identity matrix and we have defined $W = B^h B^v$, whose entries are given by:

$$W_{ij} = R_{0i}^2 \underbrace{\left(\frac{N_{hi}}{w_{hi}} \right)^2}_{\rho_i} p_{ii} p_{ji} + \sum_{\substack{k=1 \\ k \neq i}}^{N} R_{0k}^2 \underbrace{\left(\frac{N_{hi} N_{hk}}{w_{hk}^2} \right)}_{\phi_{ik}} p_{ik} p_{jk}. \tag{10}$$

R_{0i} is the local basic reproduction number for the ith patch (given by Eq. (5)), $\rho_i = N_{hi}/w_{hi}$ represents the density of residents from patch i and $\phi_{ij} = N_{hi} N_{hj}/w_{hj}^2$ is a gravitational-like term that amplifies or dampes the influence of the mobility of the residents of i.

The above result shows that the basic reproduction number is the square root of the spectral radius of the W matrix, that is:

$$R_0 = \sqrt{\rho(W)}. \tag{11}$$

It is worth noting that in the absence of mobility ($p_{11} = \cdots = p_{NN} = 1$ and $p_{ij} = 0 \, \forall i \neq j$) we get $W = diag\{R_{01}^2, \ldots, R_{0N}^2\}$ and the basic reproduction number for the metapopulation network becomes equal to the maximum of the local basic reproduction numbers R_{0i}. This reflects the fact that even in the absence of mobility, the index R_0 is able to indicate that a disease outbreak can occur in the metapopulation network although it only occurs in a single patch. As a side note, due to its relation with the risk matrix, the global R_0 (Eq. (11)) also depends on the parameters described in Table 1 throughout the local R_{0i} (Eq. (5)).

On the other hand, it is worth highlighting the case of $N = 2$ patches (Fig. 2), from which we get the following characteristic polynomial of the 2×2 matrix W:

$$p(\lambda) = \begin{vmatrix} -\lambda^2 + W_{11} & W_{12} \\ W_{21} & -\lambda^2 + W_{22} \end{vmatrix} = \lambda^4 - \lambda^2 Trz(W) + det(W),$$

where

$$W_{11} = \rho_1^2 p_{11}^2 R_{01}^2 + \phi_{12} p_{12}^2 R_{01}^2, \tag{12}$$

$$W_{12} = \rho_1^2 p_{11} p_{21} R_{01}^2 + \phi_{12} p_{12} p_{22} R_{02}^2; \tag{12}$$

and W_{22}, W_{21} are obtained by changing $1 \to 2$ in Eq. (12). Since the dwell-time parameters are always positive, the maximum eigenvalues and therefore the exact expression of R_0 for two patches is given by

$$R_0 = \sqrt{\rho(W)} = \frac{1}{\sqrt{2}} \left(Trz(W) + \sqrt{(Trz(W))^2 - 4det(W)} \right)^{1/2}. \tag{13}$$

Note that in the particular case in which there is not human mobility, i.e. $p_{12} = p_{21} = 0$ and $p_{11} = p_{22} = 1$, the risk matrix is given by $W = diag\{R_{01}^2, R_{02}^2\}$. That is, the eigenvalues of W are $\lambda_{w1} = R_{01}^2$ and $\lambda_{w2} = R_{02}^2$, which implies that $R_0 = max\{R_{01}, R_{02}\}$. On the other hand, when the mobility is extreme, that is, the residents of a given patch spend most of their time in the other patch, we have that $p_{11} \approx p_{22} \approx 0$, which implies that $p_{12} \approx p_{21} \approx 1$. According to (12), we have that $W \approx diag\{\phi_{12} R_{02}^2, \phi_{21} R_{01}^2\}$, which implies that $R_0 = max\{\sqrt{\phi_{12}} R_{02}, \sqrt{\phi_{21}} R_{01}\}$. Furthermore, in this case the gravitational-like terms are $\phi_{12} = N_{h2}/N_{h1}$ and $\phi_{21} = N_{h1}/N_{h2} = 1/\phi_{12}$, while, according to Eq. (12), the risk in patch 1 is $W_{11} = \phi_{12} R_{01}^2$ and in patch 2 is $W_{22} = R_{02}^2/\phi_{12}$. From the above expressions we corroborate that if $N_{h2} >> N_{h1}$, then the risk in patch 1 could increase while in patch 2 could decrease.

On the other hand, we propose to call W the risk matrix for the metapopulation network, since we can assess with its entries W_{ij} the secondary cases generated in patch j due to the presence of an infected human in patch i and the human mobility among patches. The above is calculated under the assumption that the residents in all the patches are in the susceptible state. It is worth mentioning that W_{ij} is similar to the basic reproduction number in the sense that it estimates the severity of the disease over the patch j due to the inclusion of an infected human in the patch i.

With the entries of the W matrix we define the risk of a vector-borne disease in patch j due to the presence of an infected human in some neighboring patch as follows:

$$\text{Risk in patch } j = \sum_{k=1}^{N} W_{kj}. \tag{14}$$

In the next section we use the expressions of R_0 for two patches (Eq. (13)) and N patches (Eq. (11)) and the patch risk (Eq. (14)) in order to analyze, numerically, the effect of the dwell-time parameter p_{ij} on the values of the basic reproduction number.
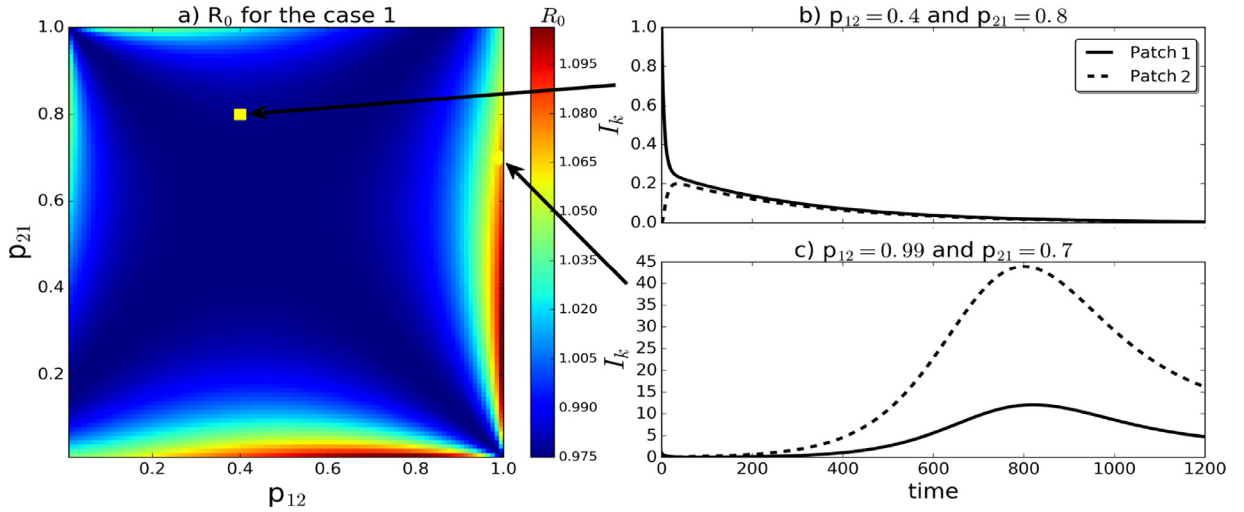
Fig. 3. (a) R_0 for the case 1 ($R_{01} = 1.04841$ and $R_{02} = 0.89536$) and for different values of the dwell-time parameters. (b) Dynamics of the infected humans in each patch with $p_{12} = 0.4$ and $p_{21} = 0.8$, from which $R_0 = 0.97662$. (c) Dynamics of the infected humans in each patch with $p_{12} = 0.99$ and $p_{21} = 0.7$, from which $R_0 = 1.119$.

4. Numerical examples

Due to the great variety of factors involved in a metapopulation network, including the topology configuration, the number of patches, the heterogeneity on the local parameters, the direction of the links, in this section we select some specific scenarios to illustrate the role of human mobility on the dynamics of the vector-borne disease. In particular we numerically analyze the two and three patches systems, and a network of patches connected in a star topology from which we obtain some conclusions that are expected to be valid for more complex topologies.

4.1. The two patches system

In order to illustrate the effect of human mobility on the disease spread of two patches (Fig. 1), in particular to the value of R_0, we assume that both subpopulations have the same number of humans ($N_{h1} = N_{h2} = 10,000$) and the same entomological parameters and human birth-mortality rates given in Table 1. Hereafter, we will use these same parameter values in all the numerical examples to define the dynamics of each patch. In what follows, we select the constant recruitment rate of vectors Λ_i (for $i = 1, 2$) according to the criteria $\Lambda_i < N_{hi}\sigma_{hi}\mu_{vi}^2/\beta_i^2$ for selecting the local basic reproduction number such that $R_{0i} < 1$; or we select $\Lambda_i > N_{hi}\sigma_{hi}\mu_{vi}^2/\beta_i^2$ to guarantee that $R_{0i} > 1$ (See Eq. (5)). The different values of the parameter Λ_i in each patch can be interpreted as a scenario with ecological diversity in the metapopulation network, where some geographical zones have better conditions for the vector reproduction (as climate, temperature, pluviosity).

We consider the following three cases of study: Case 1) without mobility, the local reproduction number of patch 1 is $R_{01} > 1$ and $R_{02} < 1$ for patch 2. This case is selected in order to look for the possibility that even if $R_{01} > 1$ the mobility could led to a global $R_0 < 1$. Case 2) both are smaller than one ($R_{01} < 1$ and $R_{02} < 1$). In this case, we analyze if the mobility could make an epidemic to appear $R_0 > 1$ even when without mobility there would not be an epidemic. Finally, case 3) both are bigger than one ($R_{01} > 1$ and $R_{02} > 1$). This case is chosen to investigate the possibility that human mobility could avoid an epidemic to appear in this extreme situation.

Case 1: We search for the existence of values for the mobility p_{ij} that could avoid an epidemic. In absence of human mobility ($p_{12} = p_{21} = 0$) this case is characterized by a potential outbreak in patch 1 ($R_{01} > 1$) but not in patch 2 ($R_{02} < 1$). Here we consider $\Lambda_1 = 55.4208$ and $\Lambda_2 = 40.4208$; using Eq. (5) we get the following values for the local reproduction number: $R_{01} = 1.04841$ and $R_{02} = 0.89536$. In Fig. 3a we show the values of R_0 (see Eq. (13)) by varying the dwell-time parameters p_{12} and p_{21} in the range [0,1].

In Fig. 3b we show the dynamics of human infections in both patches. In this example we select the dwell-time parameters $p_{12} = 0.4$ and $p_{21} = 0.8$, which according to (13), the basic reproduction number is $R_0 = 0.97662$; that is, the DFE state is stable and thus there would not be a global epidemic. Furthermore, the risk in patch 1 (defined according to Eq. (14)) is 1.00552 and for patch 2 is 0.895318. We observe that the risk index is a good indicator of local outbreaks.

As an other example of the risk index utility to predict local outbreaks, we select $p_{12} = 0.99$ and $p_{21} = 0.7$, from which $R_0 = 1.07184$; and the risk in patch 1 is 0.630716 and 1.27012 for patch 2. In Fig. 3c we can see that a disease outbreak occurs mainly in patch 2 as indicated by the risk index, even though its local basic reproduction number is less than one.

Case 2: We want to know if human mobility can led to an outbreak even if in the absence of mobility there would not be one. In this case we select $\Lambda_1 = 47.4208$ and $\Lambda_2 = 49.4208$; which according to (5), the values of the local reproduction
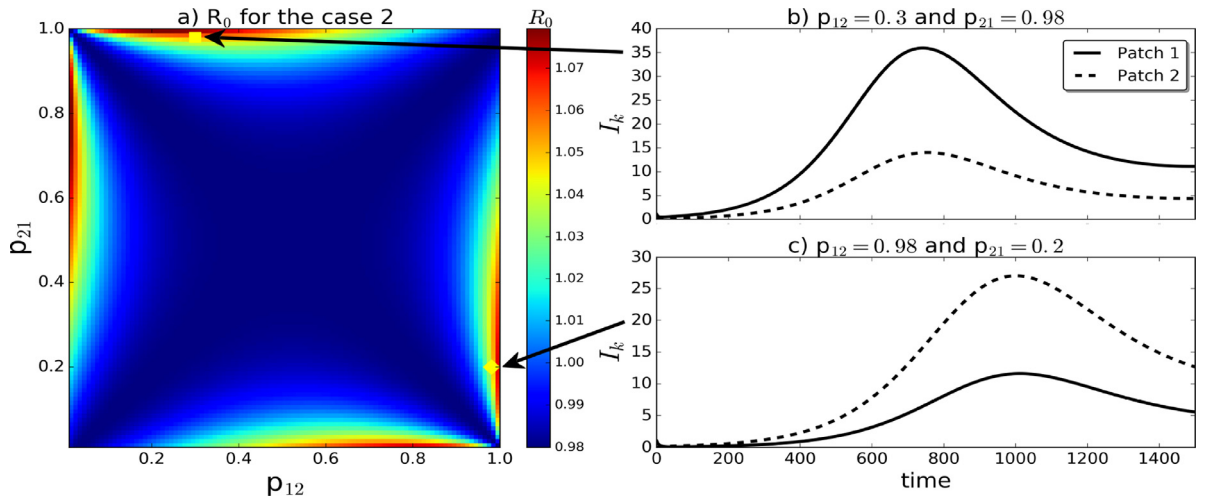
Fig. 4. (a) R_0 for the case 2 ($R_{01} = 0.9697$ and $R_{02} = 0.9900$) and for different value of the dwell-time parameters. (b) Dynamics of the infected humans in each patch with $p_{12} = 0.3$ and $p_{21} = 0.98$, from which $R_0 = 1.0614$. (c) Dynamics of the infected humans in each patch with $p_{12} = 0.98$ and $p_{21} = 0.2$, from which $R_0 = 1.0505$.
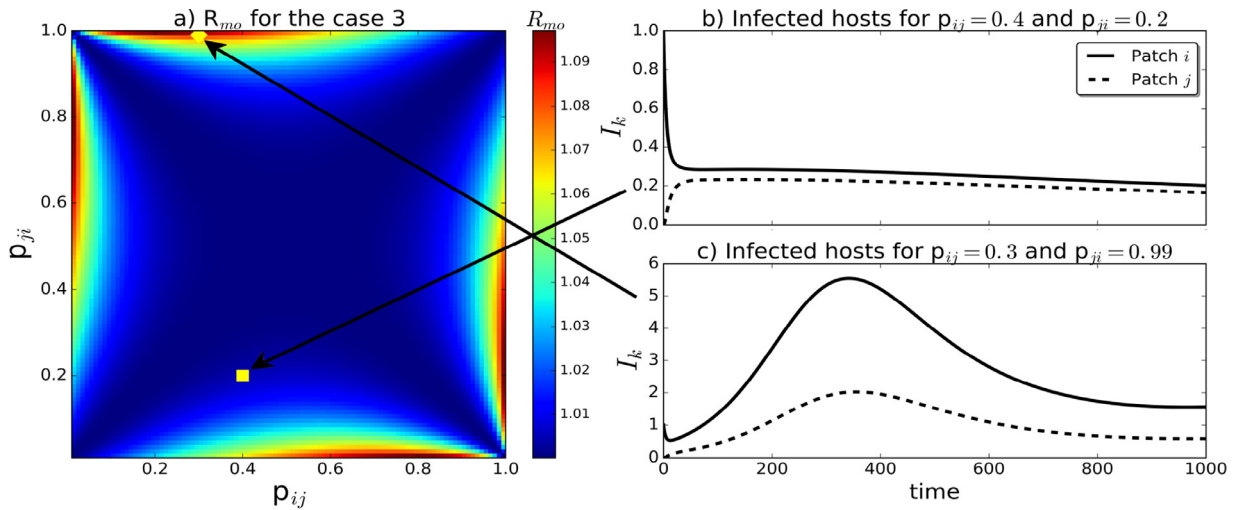

Fig. 5. (a) R_0 for the case 3 ($R_{01} = 1.0005$ and $R_{02} = 1.0002$) and for different value of the dwell-time parameters. (b) Dynamics of the infected humans in each patch with $p_{12} = 0.5$ and $p_{21} = 0.7$, from which $R_0 = 1.0012$. (c) Dynamics of the infected humans in each patch with $p_{12} = 0.97$ and $p_{21} = 0.3$, from which $R_0 = 1.0664$.

numbers are $R_{01} = 0.9697$ and $R_{02} = 0.9900$ for patch 1 and 2 respectively. In Fig. 4a we show the values of R_0 by varying the values of the dwell-time parameters in the range [0,1]. As a first example, we select $p_{12} = 0.3$ and $p_{21} = 0.98$, and using Eq. (5) we get $R_0 = 1.0614$. We thus conclude that human mobility can drive to an epidemic. Even more, by using Eq. (14) we get that the risk in patch 1 is 1.3107 and for patch 2 is 0.6098, that is, a disease outbreak is observed mainly in patch 1 as we can observe in Fig. 4b. On the other hand, by selecting $p_{12} = 0.98$ and $p_{21} = 0.2$, we get $R_0 = 1.0505$ and the largest number of infected humans occurs in patch 2 (Fig. 4c); whose risk is 1.2955 while for patch 1 is 0.6251. We observe that the local risk as defined above is a good indicator of the local severity of the outbreak.

Case 3: This set of simulations are selected to evaluate the risk index as an estimator of the epidemic severity in each patch. For this case we select $\Lambda_1 = 50.4408$ and $\Lambda_2 = 50.4708$; then, according to (5), the values of the local reproduction numbers are $R_{01} = 1.0002$ and $R_{02} = 1.0005$ for patch 1 and 2 respectively. In Fig. 5a we show the values of R_0 by varying the parameters p_{12} and p_{21} in the range [0,1]. In this case there are not values for R_0 less than one. Thus we weren't able to find a value for the mobility that can avoid a global outbreak when both local $R_{0i} > 1$. Even throw, we observe that the risk index of each patch indicates which one will be more affected by the epidemic. For example, if $p_{12} = 0.5$ and $p_{21} = 0.7$, we get from Eq. (5) that $R_0 = 1.0012$ and, the risk is 1.042 for patch 1 and 0.9589 for patch 2. On the other hand, if we select $p_{12} = 0.97$ and $p_{21} = 0.3$ we get $R_0 = 1.0664$ and the risk in patch 1 is 0.6723 and in patch 2 is 1.3290, which according to Fig. 5c, it is the patch with the highest number of infected humans.
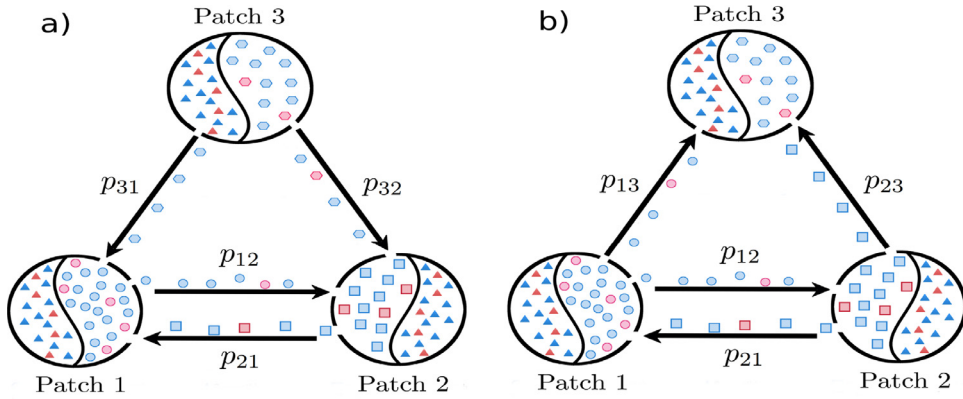
Fig. 6. The proposed scenarios for the human mobility in three connected patches. (a) An out-flow of humans of patch 3 to patch 1 and 2 is described by the dwell-time matrix P_{out}. (b) An in-flow of humans that comes from patch 1 and 2 and arrive to patch 3 is described by the dwell-time matrix P_{in}.
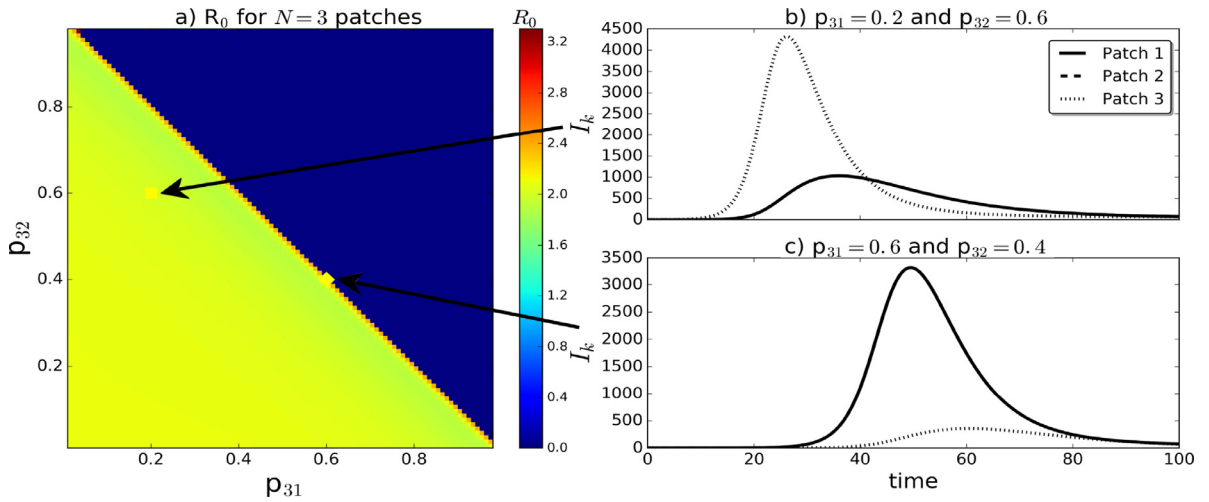

Fig. 7. (a) R_0 for $N = 3$ patches ($R_{01} = 0.7767$, $R_{02} = 0.8953$ and $R_{03} = 4.5643$) and for different values of the dwell-time parameters in the matrix P_{out}. (b) Dynamics of the infected humans in each patch with $p_{31} = 0.2$ and $p_{32} = 0.2$, from which $R_0 = 2.0215$. (c) Dynamics of the infected humans in each patch with $p_{31} = 0.6$ and $p_{32} = 0.4$, from which $R_0 = 3.2817$.

4.2. The three patches system

Here we extend the numerical analysis of two connected patches by assuming that a third one is added. In order to analyze the effect of the mobility caused by the residents of the new patch, which we label with the index 3 from now on, we assume that its local reproduction number is such that $R_{03} > 1$, while for the other patches are $R_{01} < 1$ and $R_{02} < 1$. That is, we consider that without the third patch, the DFE state for the two patches system is stable.

We propose the following two scenarios: (1) in the first one there exists an out-flow of humans of patch 3 to patch 1 and 2 (See Fig. 6a) and (2) there exists an in-flow of humans that comes from patch 1 and 2 and arrive to patch 3 (See Fig. 6b). For the first and second scenario, we propose the following dwell-time matrices:

$$P_{out} = \begin{pmatrix} 0.5 & 0.49 & 0.01 \\ 0.5 & 0.49 & 0.01 \\ p_{31} & p_{32} & p_{33} \end{pmatrix}, \quad P_{in} = \begin{pmatrix} 0.9 - p_{13} & 0.1 & p_{13} \\ 0.1 & 0.9 - p_{23} & p_{23} \\ 0 & 0 & 1 \end{pmatrix};$$

with $p_{33} = 1 - p_{31} - p_{32}$. It is worth noting that we have fixed the values of the dwell-time parameters between patches 1 and 2 such that the R_0 between them is smaller than one. Even more, for the P_{out} matrix we have assumed that $p_{13} = p_{23} = 0.01$ in order to guarantee that the value of the effective population in patch 3 (also named the patch touristic attraction w_{h3}) is a nonzero number.

In Fig. 7a we show the values of the reproduction number R_0 by assessing the spectral radius of the risk matrix (Eq. (11)) constructed with P_{out} and varying the dwell-time parameters p_{31} and p_{32} in the range [0,1]. We select the constant recruitment rate of vectors for each patch as $\Lambda_1 = 30.4208$, $\Lambda_2 = 40.4208$ and $\Lambda_3 = 1050.42$; with these values we get the following local reproduction numbers (Eq. (5)): $R_{01} = 0.7767$, $R_{02} = 0.8953$ and $R_{03} = 4.5643$. In Fig. 7b we show the dynamics
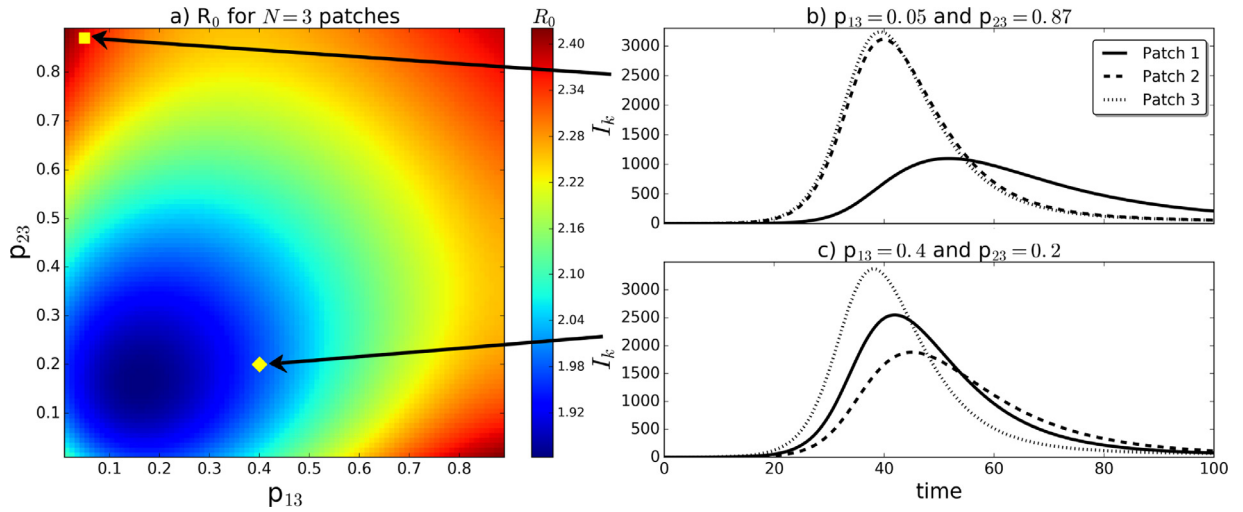
Fig. 8. (a) R_0 for $N = 3$ patches ($R_{01} = 0.9900$, $R_{02} = 0.9491$ and $R_{03} = 4.5643$) and for different values of the dwell-time parameters in the matrix P_{in}. (b) Dynamics of the infected humans in each patch with $p_{13} = 0.05$ and $p_{23} = 0.87$, from which $R_0 = 2.3713$. (c) Dynamics of the infected humans in each patch with $p_{13} = 0.4$ and $p_{23} = 0.2$, from which $R_0 = 1.9761$.
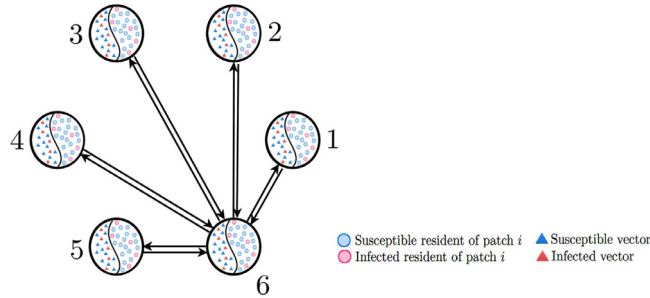

Fig. 9. A network with $N = 6$ patches connected in a star topology configuration.

of the infected humans in each patch with $p_{31} = 0.2$ and $p_{32} = 0.6$. With those values in the dwell-time parameters, the reproduction number of the three-patch system (Eq. (11)) is $R_0 = 2.02156$. The risks (Eq. (14)) in patches 1 and 2 are 0.8138 and, for patch 3 it is 5.9219 which corresponds to the patch with the highest number of infected humans. On the other hand, a major damage occurs in patch 1 and 2 when $p_{31} = 0.6$ and $p_{32} = 0.4$, from which $R_0 = 3.2817$, as we can see in Fig. 7c. It is worth noting that for these values of the dwell-time parameters, the risk (Eq. (14)) in patch 1 and 2 is 10.9185, while for the patch 3 is 0.4885. Showing again that the risk index is an indicator of local outbreak intensity.

Next we evaluate R_0 for a second example for which we use the P_{in} matrix and we select the following values of the constant recruitment rate of vector for each patch: $\Lambda_1 = 49.4208$, $\Lambda_2 = 45.4208$ and $\Lambda_3 = 1050.42$; from the above values we get the following local reproduction numbers (Eq. (5)): $R_{01} = 0.9900$, $R_{02} = 0.9491$ and $R_{03} = 4.5643$. In Fig. 8b we show the dynamics of human infections for $p_{13} = 0.05$ and $p_{23} = 0.87$, from which using Eq. (11), we get $R_0 = 2.3713$ and the risk (Eq. (14)) in patch 1 is 1.9082, in patch 2 is 5.915, and in patch 3 is 6.4373. It is worth noting that the patch 1 has the smallest risk value and for that reason, it has the smallest number of infected humans as we can see in Fig. 8b. On the other hand, in Fig. 8c we show the dynamics of human infections for $p_{13} = 0.4$ and $p_{23} = 0.2$, from which $R_0 = 1.9761$ and the risk in patch 1 is 3.6078, in patch 2 is 2.070, and in patch 3 is 6.6656. It is worth noting that in the above example, the maximum risk value corresponds to the patch with the highest number of infected humans.

4.3. A network with star topology configuration

We consider a network with $N = 6$ patches connected in a star topology configuration (see Fig. 9). Scale-free networks, for example, are characterized by the presence of central nodes (or hubs) which are connected with a great number of nodes compared with the rest of the nodes. In order to study the effect of human mobility over the disease dynamic in the metapopulation network, we consider a situation where the local reproduction number of the central patch is bigger than the rest of the patches as we describe in Table 2. Here we assume that each patch is occupied by $N_{hi} = 10,000$ (for $i = 1, \ldots, 6$) residents and we select the constant recruitment rate of vectors such that the local reproduction number in each patch is bigger than one in each patch (See Table 2). Then the introduction of an infected human in any patch will

Table 2
The selected numerical values of constant recruitment rate of vectors in each patch for the star network. We also show the corresponding values of the local reproduction numbers R_{0i} (Eq. (5)) and the patch risk (Eq. (14)) for each case explored in the numerical examples.

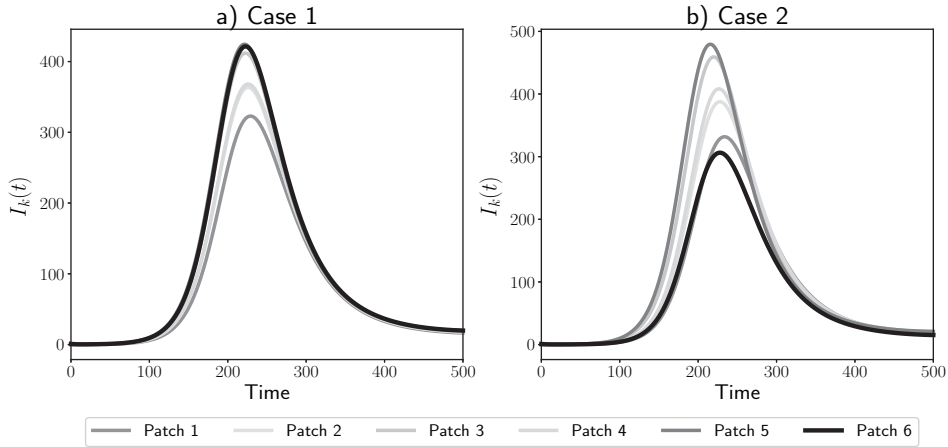| Patch	Λ_i	R_{0i}	Risk (case 1)	Risk (case 2)
1	60.421	1.094	1.386	1.414
2	65.421	1.139	1.524	1.539
3	70.421	1.182	1.754	1.770
4	75.421	1.233	1.477	1.513
5	80.421	1.263	1.728	1.736
6	180.421	1.891	1.771	1.081

Fig. 10. Disease dynamics of the model (6) for $N = 6$ patches connected in a star topology. a) case 1, where the dwell-time matrix is $P_{case\,1}$ (Eq. (15)) and b) case 2, with dwell-time matrix given by $P_{case\,2}$ (Eq. (16)).

cause a disease outbreak as we see in Fig. 10a, where we solve numerically (using the fourth order Range–Kutta method) the system (6) by introducing an infected human in the central node and using the following dwell-time matrix:

$$
P_{case\ 1} = \begin{pmatrix}
0.634 & 0 & 0 & 0 & 0 & 0.365 \\
0 & 0.546 & 0 & 0 & 0 & 0.453 \\
0 & 0 & 0.326 & 0 & 0 & 0.673 \\
0 & 0 & 0 & 0.668 & 0 & 0.331 \\
0 & 0 & 0 & 0 & 0.464 & 0.535 \\
0.1666 & 0.166 & 0.166 & 0.1666 & 0.1666 & 0.1666
\end{pmatrix}. \tag{15}
$$

With this matrix and using Eq. (11), the reproduction number R_0 of the star network is $R_0 = 1.277$ and the risk of a vector-borne disease for each patch (Eq. (14)) are given in Table 2. As we see in Fig. 10a, the central patch is the most affected by the disease outbreak since 4.214% of its population become infected (also note that it is the patch with the highest risk value), while for the patch 1 is 3.223%, for patch 2 is 3.635%, for patch 3 is 4.118%, for patch 4 is 3.682% and for patch 5 is 4.244%.

Next, by reducing the flux of the residents of patch 6 to other patches (that is, reduce p_{6i}, for $i = 1, \ldots, 5$) we can change the dynamics of human infections of the central patch as we show in Fig. 10b, where we solve numerically the system (6) with the following dwell-time matrix:

$$
P_{case\ 2} = \begin{pmatrix}
0.634 & 0 & 0 & 0 & 0 & 0.365 \\
0 & 0.546 & 0 & 0 & 0 & 0.453 \\
0 & 0 & 0.326 & 0 & 0 & 0.673 \\
0 & 0 & 0 & 0.668 & 0 & 0.331 \\
0 & 0 & 0 & 0 & 0.464 & 0.535 \\
0.0188 & 0.0188 & 0.0188 & 0.0188 & 0.0188 & 0.905
\end{pmatrix}. \tag{16}
$$

It is worth noting in Table 2 that for this second case we reduce the risk of the central patch (the patch with label 6) from 1.771 to 1.081. Even more, for this second example the central patch has the smallest value in the risk index which, according to the numerical simulation, is reflected in the fact that such patch has also the smallest value in the number of infected humans. In specific, the number of infected residents of patch 6 is 3.063%, while for the patch 1 is 3.318%, for patch

2 is 3.877%, for patch 3 is 4.592%, for patch 4 is 4.082% and for patch 5 is 4.794%. Compared with the case 1, we also reduce the reproduction number (Eq. (11)) to $R_0 = 1.258$. However, the cost of reducing the epidemic outbreak in the central patch is to increase an average of 0.484% the number of infected humans in the other patches.

5. Concluding remarks

Using a metapopulation network model with human mobility and the Next Generation Matrix (NGM) methodology, we prove that it is possible to evaluate the basic reproduction number R_0 for vector-borne diseases by calculating the spectral radius of the risk matrix W, whose dimension is $N \times N$ (with N the number of patches). The entries of W_{ij} determine the secondary infections that are generated in patch j due to the inclusion of an infected human in patch i into a complete susceptible system. The use of the matrix W reduce the computational difficulty of calculating R_0, because of in the NGM methodology it is necessary to find the spectral radius of a $2N \times 2N$ matrix. We prove that the elements of W depend on dwell-time parameters p_{ij}, the local basic reproduction numbers R_{0i}, for $i = 1, \ldots, N$ (that is, the basic reproduction number of each patch when it is not connected), the densities of humans, and the gravitational-like term $N_{hi}N_{hj}/w_{hj}^2$, where N_{hi} and w_{hi} are the number of residents and the tourist attraction of the ith patch, respectively.

We relate the matrix W with a risk index based in [17]. This index can be used to locally evaluate the vulnerability of each patch, while the R_0 can be used to estimate the disease damage globally. Using these theoretical results, we numerically study the parametric sensitivity of R_0 with respect to the dwell-time parameters p_{ij}. By means of particular cases we found two non trivial effects on R_0 due to mobility. The first one is that even if the local R_{0i} of the patches is less than one, human mobility can led to a global R_0 greater than one. The second one is that even if one local R_{0i} is greater than one, particular values of the mobility led to a global R_0 less than one. This suggests that in a disconnected stable scenario, i.e. $R_{0i} < 1$, $\forall i$, some structures of human mobility can trigger a disease outbreak in the metapopulation network ($R_0 > 1$). On the contrary, in an unstable disconnected scenario, i.e. $\exists\, i$ such that $R_{0i} > 1$, human mobility can dampen the disease outbreak ($R_0 < 1$). Furthermore, we observe that for a metapopulation network connected in a star topology configuration, it is also possible to reduce the number of infected humans in the most connected patch by decreasing the flux of humans that leave the patch.

Acknowledgments

References

[1] Carvalho FD, Moreira LA. Why is aedes aegypti linnaeus so successful as a species? Neotropical Entomol 2017;46(3):243–55.
[2] Kraemer MUG, Sinka ME, Duda KA, Mylne A, Shearer FM, Barker CM, Moore CG, Carvalho RG, Coelho GE, Bortel WV, Hendrickx G, Schaffner F, Elyazar IR, Teng HJ, Brady OJ, Messina JP, Pigott DM, Scott TW, Smith DL, Wint GW, Golding N, Hay SI. The global distribution of the arbovirus vectors Aedes aegypti and Ae. albopictus. eLife 2015;4:E08347.
[3] World Health Organization. Zika Situation Report. Technical Report, World Health February 2016;.
[4] World Health Organization. Chikungunya Fact Sheet n327. 2017. http://www.who.int/news-room/fact-sheets/detail/chikungunya.
[5] Bichara D, Castillo-Chavez C. Vector-borne diseases models with residence times a Lagrangian perspective. Math Biosci 2016;281:128–38.
[6] Alberto MYA, Andreia NSH, Sandro M, Chiara P, Vittoria C. Human mobility networks and persistence of rapidly mutating pathogens. R Soc Open Sci 2017;4:160914.
[7] Brockmann D. Human mobility and spatial disease dynamics. Rev Nonlinear Dyn Complex 2010;2:1–24.
[8] Cosner C, Beier JC, Cantrell RS, Impoinvil D, Kapitanski L, Potts MD, Troyo A, Ruan S. The effects of human movement on the persistence of vector-borne diseases. J Theor Biol 2009;258(4):550–60.
[9] Manore CA, Hickmann KS, Hyman JM, Foppa IM, Davis JK, Wesson DM, Mores CN. A network-patch methodology for adapting agent-based models for directly transmitted disease to mosquito-borne disease. J Biol Dyn 2015;9(1):5272. doi:10.1080/17513758.2015.1005698.
[10] Keeling MJ, Rohani P. Modeling infectious diseases in humans and animals. 1st ed. Princeton University Press; 2007.
[11] Massaro E, Ganin A, Perra N, Linkov I, Vespignani A. Resilience management during large-scale epidemic outbreaks. Sci Rep 2018;8:1–9.
[12] Gómez-Gardeñes J, Soriano-Paños D, Arenas A. Critical regimes driven by recurrent mobility patterns of reaction–diffusion processes in networks. Nat Phys 2017;14:391–5.
[13] Quian VAZ, Kaiyuan S, Matteo C, Ana PyP, Dean Natalie E, Diana PR, Stefano M, Dina M, Piero P, Luca R, Margaret B, Elizabeth HM, Longine Ira M. Spread of Zika virus in the americas. PNAS 2017;114(22):E4334–43.
[14] Hanski I. Metapopulation dynamics. Nature 1998;396(6706):41–9.
[15] Arino J, van den Driessche P. A multi-city epidemic model. Math Popul Stud 2003;10(3):175–93.
[16] Moulay D, Pigné Y. A metapopulation model for Chikungunya including populations mobility on a large-scale network. J Theor Biol 2013;318:129–39.
[17] Velázquez-Castro J, Anzo-Hernández A, Bonilla-Capilla B, Soto-Bajo M, Fraguela-Collar A. Vector-borne disease risk indexes in spatially structured populations. PLOS Negl Trop Dis 2018. doi:10.1371/journal.pntd.0006234.
[18] Heesterbeek JAP. A brief history of R0 and a recipe for its calculation. Acta Biotheoretica 2002;50(3):189–204. http://www.who.int/news-room/fact-sheets/detail/chikungunya.
[19] Brauer F, Castillo-Chavez C. Epidemic models. In: Mathematical models in population biology and epidemiology, 40. Springer; 2010. p. 393–403. ch. 9
[20] Diekmann O, Heesterbeek JAP, Roberts MG. The construction of next-generation matrices for compartmental epidemic models. J R Soc Interf 2010;7(47):873–85.
[21] Iggidr ASM, Koiller J, Penna MLF, Sallet G, Silva MA. Vector borne diseases on an urban environment: the effects of heterogeneity and human circulation. Ecol Complex 2017;3:76–90.

[22] Lee C, Sunmi C-C. The role of residence times in two-patch dengue transmission dynamics and optimal strategies. J Theor Biol 2015;374:152–64. June 2015.

[23] Pliego EP, Velázquez-Castro J, Collar AF. Seasonality on the life cycle of Aedes aegypti mosquito and its statistical relation with dengue outbreaks. Appl Math Model 2017;50:484–96.

[24] Adams B, Boots M. How important is vertical transmission in mosquitoes for the persistence of dengue? Insights from a mathematical model. Epidemics 2010;2(1):1–10.

[25] Erickson RA, Presley SM, Allen LJS, Long KR, Cox SB. A dengue model with a dynamic Aedes albopictus vector population. Ecol Model 2010;221(24):2899–908.

[26] Martcheva M. Techniques for computing ro. In: An Introduction to Mathematical Epidemiology. Springer US; 2015. p. 104–16. ch. 5.

[27] Powell DP. Calculating determinants of block matrices, 2011. arXiv:1112.4379.

[28] Silvester J. Determinants of block matrices. Math Gaz 2000;8(501):460–7.